Hindawi
Journal of Applied Mathematics
Volume 2022, Article ID 2799773, 11 pages
https://doi.org/10.1155/2022/2799773

Research Article

Effects of Slip and Inclined Magnetic Field on the Flow of Immiscible Fluids (Couple Stress Fluid and Jeffrey Fluid) in a Porous Channel

Punnamchandar Bitla and Fekadu Yematow Sitotaw

Department of Mathematics, College of Natural and Computational Sciences, Wollega University, Nekemte, Ethiopia

Correspondence should be addressed to Punnamchandar Bitla; punnam.nitw@gmail.com

Received 14 June 2022; Revised 24 August 2022; Accepted 29 August 2022; Published 22 September 2022

Academic Editor: Oluwole D. Makinde

In this paper, we study the flow of two immiscible fluids namely, couple stress fluid and Jeffrey fluid in a porous channel. Instead of the classical no-slip conditions on the boundaries, we used slip boundary conditions, which are more realistic and meaningful. In addition, we used inclined magnetic field effects on the fluid flow. The couple stress fluid and Jeffrey fluid are flowing adjacent to each other in the region I and in the region II, respectively, of the horizontal porous channel. The nondimensionalized governing equations are solved analytically by using slip conditions at the lower and upper boundaries and interface conditions at the fluid-fluid interface. The analytical expressions for the velocity components in both regions are obtained in closed form. The effects of slip parameter, Hartmann number, couple stress parameter, Jeffrey parameter, angle of inclination, and Darcy number on velocity components in both regions are investigated. In the absence of slip, couple stress parameter, and Jeffrey parameters, limiting cases are obtained and discussed.

1. Introduction

As the classical Newtonian fluid theory is inadequate to explain the fluids with additives and other nonlinear stress and strain relationships that occur in real fluids, many non-Newtonian fluid theories are proposed. Non-Newtonian fluids are categorized as visco-elastic fluids, time-dependent fluids, and time-independent fluids [1, 2].

Stokes [3] in 1966 proposed the couple stress theory by introducing the nonsymmetry of the stress tensor that shows the effects of couple stresses. This fluid theory gained the attention of researchers due to its major applications in lubrication theory, liquid crystals, blood flows, etc. A review of couple stress fluid dynamics was reported by Stokes [4] in 1984. The presence of couple stress parameter decreases the velocity of the fluid and other parameters effect on the velocity of a single couple stress fluid studied by Devakar et al. [5], Ahmad [6], and Jangili et al. [7].

Other non-Newtonian fluid which has been attracted much by the researchers in view of its simplicity is known as Jeffrey fluid [8]. The Jeffrey fluid model is able to describe the characteristics of relaxation and retardation time. Jeffrey's fluid model is a significant generalization of the Newtonian fluid model as the latter one can be deduced as a special case of the former. Several scholars have studied Jeffrey fluid flow under different assumptions and conditions. Akbar et al. [9] have studied the effect of thermal and velocity slip for Jeffrey fluid symmetric channel. Akram and Nadeem [10] studied analytically the influence of induced magnetic field on the peristaltic motion of a Jeffrey fluid in an asymmetric channel. Shail [11] studied theoretically the possibility of using a two-phase system to obtain increased flow rates in an electromagnetic pump. Meyer and Garder [12] analyzed the mechanics of two immiscible fluids in porous media. Bhattacharya [13] studied the flow of immiscible fluids in a rigid channel with a time-dependent pressure gradient.

The study of immiscible fluids like Newtonian versus Newtonian, Newtonian versus Non-Newtonian, and/or Non-Newtonian versus Non-Newtonian fluids occurs in industries, manufacturing process, groundwater hydrology, etc. Recently, several researchers studied the flows of immiscible fluids, to mention a few, such as Newtonian fluid-Newtonian fluid or Newtonian-Non-Newtonian fluid (Berg et al. [14], Padma Devi and Srinivas [15], Yadav and Sneha [16, 17], Deo and Ansari [18], Matias et al. [19], Malashetty and Umavathi [20], Ramana Murthy and Srinivas [21], and Punnamchandar and Fekadu [22]) in channel configurations with slip and/or no-slip boundary conditions.

In general, the no-slip boundary condition is used when the fluid flows past rigid boundaries. However, it has been accepted now that a number of fluids such as polymerics and additive fluids slip/stick-slip on rigid boundaries. To describe the slip characteristics of a fluid on the solid surface, "*Navier introduced a more general boundary condition – that the fluid velocity component tangential to the solid surface, relative to the solid surface, is proportional to the shear stress on the fluid-solid interface*" (Thompson and Troia [23]). *"Recent advances in experimental and mathematical investigation and results have provided evidence in support of the slip condition and try to show its effects on different fluid model*" (Akram et al. [24], Punnamchandar and Iyengar [25], Ashmawy [26], and Srinivasacharya and Bindu [27]).

To the extent, the authors have surveyed the combined effects of slip and inclined magnetic field on the flow of immiscible couple stress fluid and Jeffrey fluids in a porous medium channel have not been studied. Hence, in this paper, the flow of two immiscible fluids in a porous medium channel with an inclined magnetic field along with the slip at the boundaries is analyzed. The analytical expressions for the velocity components in both regions are obtained in closed form. The effects of various parameters on the two velocity profiles are shown graphically and briefly discussed.

2. Mathematical Formulation of the Problem

Consider a fully developed laminar incompressible, immiscible couple stress, and Jeffrey fluids flow through a porous medium between two parallel horizontal plates which are 2 h distance apart. The x-axis is taken in the midway direction of the porous channel, and the y-axis is taken normal to the porous channel (Figure 1).

Let β_1 and β_2 be the slip coefficients of the fluids at the lower and the upper plates of the channel, respectively. The fluid flow is driven by a common pressure gradient. The couple stress fluid in the region I $(-h \le y \le 0)$ has density ρ_1, shear viscosity μ_1, and couple stress viscosity η_1. Similarly, the Jeffrey fluid in the region II $(0 \le y \le h)$ has density ρ_2, shear viscosity μ_2 and λ_1 is the material parameter of a Jeffrey fluid. The porous medium is rigid, isotropic, and homogeneous with permeabilitiesk_1 and k_2 in the two regions, respectively.

A uniform magnetic field $B_o$is applied at an inclined angleθ with respect to the positive y-direction. The couple stress fluid and Jeffrey fluid are assumed to be slightly conducting. Hence, the induced magnetic field is negligible in comparison to the applied uniform inclined magnetic field. The Lorentz force is the only body force acting on the fluid, and there are no body couples.

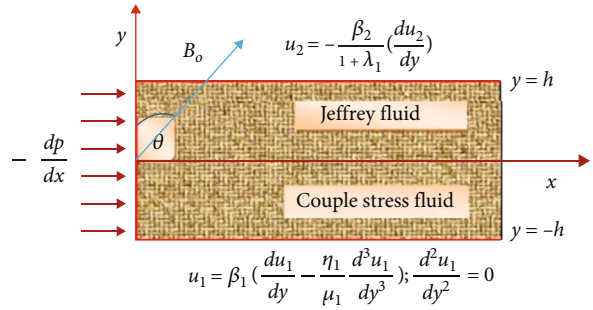

FIGURE 1: A schematic representation of the flow of two immiscible fluids.

For region I $(-h \le y \le 0)$,

following Stokes [3] and Skelland [1], the flow of couple stress fluid in the region I has an extra stress tensor compare with Navier - Stokes equation is governed by the differential equations given by

$$\mu_1 \frac{d^2u_1}{dy^2} - \eta_1 \frac{d^4u_1}{dy^4} - \sigma_1 B_o^2 \cos^2\theta u_1 - \frac{\mu_1}{k_1} u_1 = -\frac{dp}{dx}. \quad (1)$$

For region II $(0 \le y \le h)$,

following Chabra and Richardson [2], Akbar et al. [9], and Akram and Nadeem [10], the flow of Jeffrey fluid in region II has an extra stress tensor $S = \mu_2/1 + \lambda_1(\dot{\gamma} + \ddot{\gamma})$, $\dot{\gamma}$ is the shear rate. Using the above assumptions and this extra stress tensor, the governing differential equation reduced to

$$\frac{\mu_2}{1+\lambda_1} \frac{d^2u_2}{dy^2} - \sigma_2 B_0^2 \cos^2\theta u_2 - \frac{\mu_2}{k_2} u_2 = -\frac{dp}{dx}, \quad (2)$$

where dp/dx represents the driving force i.e., the common pressure gradient, $\mu_i d^2u_i/dy^2$ represents the force due to shear stresses, $\eta_1 d^4u_1/dy^4$ represents the force due to couple stresses, $\sigma_i B_o^2 u_i$ represent the Lorentz force due to applied magnetic field, $\mu_i/k_i u_i$ represents the retarding force due to porous media in both the fluid regions.

To determine the velocity field components $u_1(y)$ and $u_2(y)$ in region I and region II described above, we adopt the following boundary and interface conditions:

(i) at $y = -h$, the Navier slip relation says that the shear stress on the fluid at the boundary is proportional to the fluid velocity at the boundary [28]. A velocity slip boundary condition proposed by Navier in which slip velocity depends upon shear stress. Devakar et al. [5] and Pei-Ying et al. [29] presented the analytical solution for a couple stress fluids by taking velocity slip conditions. This slip conditions is given by

$$u_1 = \beta_1 \left(\frac{du_1}{dy} - \frac{\eta_1}{\mu_1} \frac{d^3 u_1}{dy^3} \right). \tag{3}$$

Stokes [3] has proposed two types of boundary Conditions (A) and (B), respectively, and the vanishing of couple stresses on the boundary is referred to as Condition (A). This condition is adopted here as this is appropriate in the present context. The vanishing of couple stresses is given by

$$\frac{d^2 u_1}{dy^2} = 0. \tag{4}$$

(ii) at $y = 0$, at the fluid–fluid interface, Murthy and Srinivas [21] assumed that the velocity, shear stress, and couple stress components are continuous. This implies:

Continuity of velocities,

$$\begin{aligned} \mathrm{u}_1(0^-) &= \mathrm{u}_2(0^+), \\ u_1 &= u_2. \end{aligned} \tag{5}$$

Vanishing of couple stresses,

$$\begin{aligned} \mathrm{M}_{\mathrm{xy}}\big|_1(0^-) &= \mathrm{M}_{\mathrm{xy}}\big|_2(0^+), \\ \frac{d^2 u_1}{dy^2} &= 0. \end{aligned} \tag{6}$$

Continuity of shear stresses,

$$\begin{aligned} \tau_{\mathrm{xy}}\big|_1(0^-) &= \tau_{\mathrm{xy}}\big|_2(0^+), \\ \left(\mu_1 \frac{du_1}{dy} - \eta_1 \frac{d^3 u_1}{dy^3} \right) &= \left(\frac{\mu_2}{1+\lambda_1} \right) \frac{du_2}{dy}. \end{aligned} \tag{7}$$

(iii) at $y = h$, the slip boundary condition for Jeffrey fluid, is given by (Ramesh [30])

$$u_2 = -\frac{\beta_2}{(1+\lambda_1)} \frac{du_2}{dy}, \tag{8}$$

By introducing the nondimensional quantities, $x^* = x/h$, $y^* = y/y$, $u_i^* = u_i/U$, $p^* = p/\rho_1 U^2$ where U is the maximum velocity of the fluid in the channel and $i = 1, 2$, we have the governing equations, boundaries, and interface conditions (in the nondimensionalized form after dropping $*$'s) as

For region I $(-1 \le y \le 0)$,

$$\frac{1}{\mathrm{s}_1} \frac{d^4 u_1}{dy^4} - \frac{d^2 u_1}{dy^2} + \left(M^2 + \frac{1}{Da} \right) u_1 = \mathrm{Re}\ P. \tag{9}$$

Similarly for region II $(0 \le y \le 1)$,

$$\frac{1}{1+\lambda_1} \frac{d^2 u_2}{dy^2} - \left(\frac{1}{K\,Da} + \frac{n_\sigma}{n_\mu} M^2 \right) u_2 = -\frac{n_\rho}{n_\mu}\ \mathrm{Re}\ P. \tag{10}$$

(i) at $y = -1$,

$$\begin{aligned} u_1 &= \frac{1}{\alpha_1} \left(\frac{du_1}{dy} - \frac{1}{s_1} \frac{d^3 u_1}{dy^3} \right), \\ \frac{d^2 u_1}{dy^2} &= 0 \end{aligned} \tag{11}$$

(ii) at $y = 0$,

$$\begin{aligned} u_1 &= u_2 \\ \frac{n_\mu}{1+\lambda_1} \left(\frac{du_2}{dy} \right) &= \frac{du_1}{dy} - \frac{1}{s_1} \frac{d^3 u_1}{dy^3}, \\ \frac{d^2 u_1}{dy^2} &= 0 \end{aligned} \tag{12}$$

(iii) at $y = 1$,

$$u_2 = -\frac{1}{(1+\lambda_1)\alpha_2} \left(\frac{du_2}{dy} \right), \tag{13}$$

where $P = -dp/dx$ is the constant pressure gradient, $\mathrm{Re} = \rho_1 U h/\mu_1$ is the Reynolds number, $\alpha_i = h/\beta_i (i = 1, 2)$ are the slip parameters, $s_1 = \mu_1 h^2/\eta_1$ is the couple stress parameter, $Ha = B_0 h \sqrt{\sigma/\mu_1}$ is the Hartmann number, $M = Ha\,Co\,s\theta$, $Da = k/h^2$ is the Darcy number, $n_\sigma = \sigma_2/\sigma_1$ is the electric conductivity ratio, $n_\mu = \mu_2/\mu_1$ is the viscosity ratio, and $n_\rho = \rho_2/\rho_1$ is the density ratio.

3. Solution of the Problem

Region I $(-1 \le y \le 0)$, from Equation (9), the velocity component differential equation in region I is given by

$$\begin{aligned} u_1(y) = {} & C_{11} \cosh \lambda_{11} y + C_{12} \sinh \lambda_{11} y \\ & + C_{13} \cosh \lambda_{12} y + C_{14} \sinh \lambda_{12} y + \mathrm{P1} \end{aligned}$$

where $\lambda_{1i} = (-1)^{i-1} \sqrt{\mathrm{s}_1/2 \pm 1/2 \sqrt{\mathrm{s}_1{}^2 - 4\mathrm{m}_1}}$, $i = 1, 2$,

$$m_1 = \left(M^2 + \frac{1}{Da} \right) s_1 \,;\ \mathrm{P1} = \frac{\mathrm{Re}\ P s_1}{m_1}. \tag{15}$$

Region II ($0 \le y \le 1$), from Equation (10), the velocity component differential equation in region II is given by

$$u_2(y) = C_{21} \cosh \lambda_{21} y + C_{22} \sinh \lambda_{21} y + P2, \tag{16}$$

where $\lambda_{2i} = (-1)^{i-1} \sqrt{m_2}$ for $i = 1, 2$,

$$m_2 = \left(\frac{\eta_\sigma}{\eta_\mu} M^2 + \frac{1}{K\,Da}\right)(1 + \lambda_1),$$
$$P2 = \frac{n_\rho}{n_\mu m_2}(1 + \lambda_1)\ \mathrm{Re}\ P. \tag{17}$$

The velocity components $u_1(y)$ and $u_2(y)$ involve six constants $C_{11}, C_{12}, C_{13}, C_{14}, C_{21}$, and C_{22}. The expressions of these are given in appendix A.

Evaluation of volumetric flow rate : the expression of volumetric flow rate through the channel in dimensionless form can be evaluated using the following relation [31]:

$$Q(y) = \int_{-1}^{0} u_1(y)dy + \int_{0}^{1} u_2(y)dy,$$
$$\begin{aligned} Q(y) = {} & \frac{\sinh \lambda_{11}}{\lambda_{11}} C_{11} + \frac{(1 - \cosh \lambda_{11})}{\lambda_{11}} C_{12} + \frac{\sinh \lambda_{12}}{\lambda_{12}} C_{13} \\ & + \frac{(1 - \cosh \lambda_{12})}{\lambda_{12}} C_{14} + P1 + \frac{\sinh \lambda_{21}}{\lambda_{21}} C_{21} \\ & + \frac{(\cosh \lambda_{21} - 1)}{\lambda_{21}} C_{22} + P2. \end{aligned} \tag{18}$$

Evaluation of shearing stress : the expression for nondimensional shearing stress experienced by fluids in the upper and lower region of the horizontal porous channel [31], respectively, is given by:

Therefore, the general solution is given by

$$\begin{aligned} u_1(y) = {} & C_{11} \cosh \lambda_{11} y + C_{12} \sinh \lambda_{11} y + C_{13} \cosh \lambda_{12} y \\ & + C_{14} \sinh \lambda_{12} y + P1, \end{aligned} \tag{21}$$

where $\lambda_{1i} = (-1)^{i-1} \sqrt{s_1/2 \pm 1/2\sqrt{s_1^2 - 4m_1}}$ for $i = 1, 2$.

4. Particular Solution for the Effects of Slip and Inclined Magnetic Field on the Immiscible Fluid Flow in a Horizontal Porous Channel

4.1. Immiscible Fluids (CSF and Newtonian Fluid) Flow in the Assumed Channel in the Existence of a Uniform Inclined Magnetic Field for $\lambda_1 = 0$. Region I ($-1 \le y \le 0$), the governing differentialequation is given by

$$\frac{1}{s_1}\frac{d^4 u_1}{dy^4} - \frac{d^2 u_1}{dy^2} + \left(M^2 + \frac{1}{Da}\right) u_1 = \mathrm{Re}\ P. \tag{20}$$

$$\left.\begin{aligned} \tau_{xy1} &= \frac{du_1}{dy} - \frac{1}{s_1}\frac{d^3 u_1}{dy^3}\ at\ y = -1, \\ \tau_{xy2} &= -\frac{1}{(1 + \lambda_1)}\frac{du_2}{dy}\ at\ y = 1. \end{aligned}\right\}$$

$$\left.\begin{aligned} \tau_{xy1} = {} & C_{12}\left((\cosh \lambda_{11})\lambda_{11} - \frac{(\cosh \lambda_{11})\lambda_{11}^3}{s_1}\right), \\ & C_{11}\left(-(\sinh \lambda_{11})\lambda_{11} + \frac{(\sinh \lambda_{11})\lambda_{11}^3}{s_1}\right), \\ & + C_{14}\left((\cosh \lambda_{12})\lambda_{12} - \frac{(\cosh \lambda_{12})\lambda_{12}^3}{s_1}\right), \\ & + C_{13}\left(-(\sinh \lambda_{12})\lambda_{12} + \frac{(\sinh \lambda_{12})\lambda_{12}^3}{s_1}\right), \\ \tau_{xy2} = {} & -\frac{1}{(1 + \lambda_1)}((\sinh \lambda_{21})C_{21}\lambda_{21}), \\ & -\frac{1}{(1 + \lambda_1)}((\sinh \lambda_{21})C_{22}\lambda_{21}). \end{aligned}\right\} \tag{19}$$

Region II ($0 \le y \le 1$), the governing differential equation is given by

$$\frac{d^2u_2}{dy^2} - \left(\frac{1}{K\,Da} + \frac{n_\sigma}{n_\mu}M^2\right)u_2 = -\frac{n_\rho}{n_\mu}\ \mathrm{Re}\ P. \tag{22}$$

Therefore, the general solution is given by

$$u_2(y) = C_{21}\cosh\lambda_{21}y + C_{22}\sinh\lambda_{21}y + P2, \tag{23}$$

where $\lambda_{21} = \sqrt{m_2}$; $m_1 = (M^2 + 1/Da)s_1$, $P1 = \mathrm{Re}\ P\,s_1/m_1$,

$$m_2 = \left(\frac{\eta_\sigma}{\eta_\mu}M^2 + \frac{1}{K\,Da}\right),\ P2 = \frac{n_\rho}{n_\mu m_2}\ \mathrm{Re}\ P. \tag{24}$$

4.2. Immiscible Newtonian and Jeffery Fluids Flow in the Assumed Channel in the Existence of a Uniform Inclined Magnetic Field for $\eta_1 = 0$ or $s_1 \longrightarrow \infty$. Region I ($-1 \le y \le 0$), the governing differential equation is given by

$$-\frac{\mathrm{d}^2\mathrm{u}_1}{\mathrm{dy}^2} + \left(Ha^2 + \frac{1}{Da}\right)\mathrm{u}_1 = \mathrm{Re}\ P. \tag{25}$$

Therefore, the general solution is given by

$$u_1(y) = C_{11}\cosh\lambda_{11}y + C_{12}\sinh\lambda_{11}y + P1. \tag{26}$$

Region II ($0 \le y \le 1$), the governing differential equation is given by

$$\frac{1}{1+\lambda_1}\frac{d^2u_2}{dy^2} - \left(\frac{1}{K\,Da} + \frac{n_\sigma}{n_\mu}M^2\right)u_2 = -\frac{n_\rho}{n_\mu}\ \mathrm{Re}\ P. \tag{27}$$

Therefore, the general solution is given by

$$u_2(y) = C_{21}\cosh\lambda_{21}y + C_{22}\sinh\lambda_{21}y + P2 \tag{28}$$

where $\lambda_{11} = \sqrt{m_1}$; $\lambda_{2i} = (-1)^{i-1}\sqrt{m_2}$ for $i = 1, 2$, $m_1 = (M^2 + 1/Da)$, $m_2 = (\eta_\sigma/\eta_\mu M^2 + 1/K\,Da)(1 + \lambda_1)$, $P1 = (\mathrm{Re}\ P)/m\_1$, and $P2 = n\_\rho/(n\_\mu\, m\_2)\,(1 + \lambda\_1)\ \mathrm{Re}\ P$.

4.3. Immiscible Newtonian and Newtonian Fluid Flow in the Channel in the Existence of Uniform Inclined Magnetic Field for $\eta_1 = 0$ or $s_1 \longrightarrow \infty$ and $\lambda_1 = 0$. Region I ($-1 \le y \le 0$), the governing differential equation is given by

$$-\frac{\mathrm{d}^2\mathrm{u}_1}{\mathrm{dy}^2} + \left(M^2 + \frac{1}{Da}\right)\mathrm{u}_1 = \mathrm{Re}\ P. \tag{29}$$

Therefore, the general solution is given by

$$u_1(y) = C_{11}\cosh\lambda_{11}y + C_{12}\sinh\lambda_{11}y + P1. \tag{30}$$

Region II ($0 \le y \le 1$), the governing differential equation is given by

$$\frac{d^2u_2}{dy^2} - \left(\frac{1}{K\,Da} + \frac{n_\sigma}{n_\mu}M^2\right)u_2 = -\frac{n_\rho}{n_\mu}\ \mathrm{Re}\ P. \tag{31}$$

Therefore, the general solution is given by

$$u_2(y) = C_{21}\cosh\lambda_{21}y + C_{22}\sinh\lambda_{21}y + P2, \tag{32}$$

where $\lambda_{11} = \sqrt{\mathrm{m}_1}$, $\lambda_{21} = \sqrt{\mathrm{m}_2}$, $m_1 = (M^2 + 1/Da)$, $P1 = \mathrm{Re}\ P/m_1$, $m_2 = (\eta_\sigma/\eta_\mu M^2 + 1/K\,Da)$, and $P2 = n_\rho/n_\mu m_2\ \mathrm{Re}\ P$.

4.4. Comparative Study with Kumar and Agarwal [32]. Assuming the two immiscible fluids are Newtonian fluids in such a way that the fluid in region I is nonconducting and the fluid in region II is conducting fluids. From our model equation given in Equations (1) and (2), let the couple stress viscosity is zero ($\eta_1 = 0$ or $s_1 \longrightarrow \infty$), and the Jeffrey fluid parameter is also zero ($\lambda_1 = 0$), and the angle of inclination $\theta = 0$ (which implies $M = Ha$) then we have the following.

Region I ($-1 \le y \le 0$), the differential equation is given by

$$-\frac{\mathrm{d}^2\mathrm{u}_1}{\mathrm{dy}^2} + \left(\mathrm{Ha}^2 + \frac{1}{\mathrm{Da}}\right)\mathrm{u}_1 = \mathrm{Re}\ P. \tag{33}$$

Therefore, the general solution is given by

$$u_1(y) = C_{11}\cosh\lambda_{11}y + C_{12}\sinh\lambda_{11}y + P1. \tag{34}$$

Region II ($0 \le y \le 1$), the differential equation is given by

$$\frac{d^2u_2}{dy^2} - \left(\frac{1}{Da}\right)u_2 = -\frac{n_\rho}{n_\mu}\ \mathrm{Re}\ P. \tag{35}$$

Therefore, the general solution is given by

$$u_2(y) = C_{21}\cosh\lambda_{21}y + C_{22}\sinh\lambda_{21}y + P2, \tag{36}$$

where $\lambda_{11} = \sqrt{\mathrm{m}_1}$; $\lambda_{21} = \sqrt{\mathrm{m}_2}$; $m_1 = (Ha^2 + 1/Da)$,

$$P1 = \frac{\mathrm{Re}\ P}{m_1};\ m_2 = \left(\frac{1}{Da}\right);\ P2 = \frac{n_\rho}{n_\mu m_2}\ \mathrm{Re}\ P. \tag{37}$$

Now by sustitutingthe following variables in to the equations(34) and (36) ($P = P_s$, $Ha = M$, $Da = K$, and $n_\mu = 1/\beta$;

$$n_\rho = \frac{1}{\alpha},\ m_1 = A_1,\ m_2 = A_2,\ \mathrm{Re} = R_1,\ C_{11} = C_1, \tag{38}$$

$C_{12} = C_2$, $C_{21} = C_3$, and $C\ 22 = C_4$), after simplification

$$u_1(y) = C_1\cosh\sqrt{A_1}y + C_2\sinh\sqrt{A_1}y + \frac{\mathrm{Re}_1\mathrm{P}_\mathrm{s}}{A_1}, \tag{39}$$

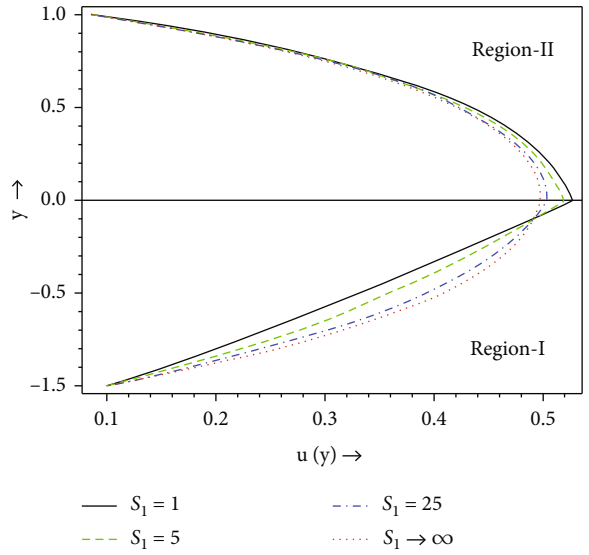

FIGURE 2: Effect of couple stress parameter S_1 on velocity components.

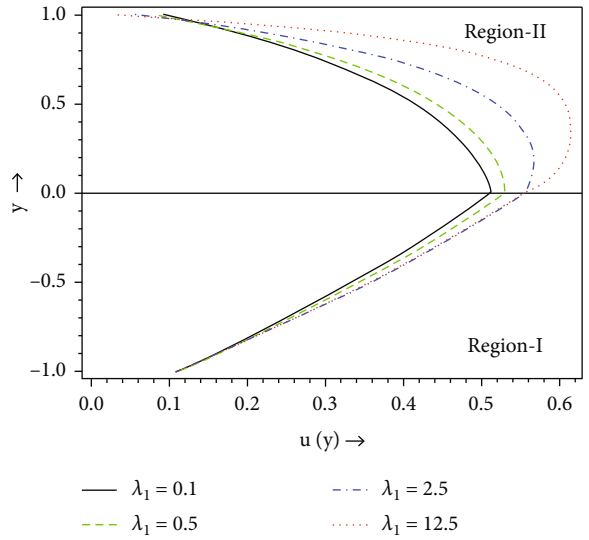

FIGURE 3: Variation of velocity profile with Jeffrey parameter λ_1.

$$u_2(y) = C_3 \cosh \sqrt{A_2}y + C_4 \sinh \sqrt{A_2}y + \frac{\alpha R_1 P_s}{A_2}. \quad (40)$$

These equations (39) and (40) are exactly the same with the work of Kumar and Agarwal [32] which is the solution of steady flow.

5. Results and Discussion

5.1. Velocity Profile. The flow of immiscible fluids (couple stress fluid and Jeffery fluid) in a horizontal porous channel in the presence of a uniform inclined magnetic field is considered. The simplified model equations are solved analytically, and the expressions for velocities in both are

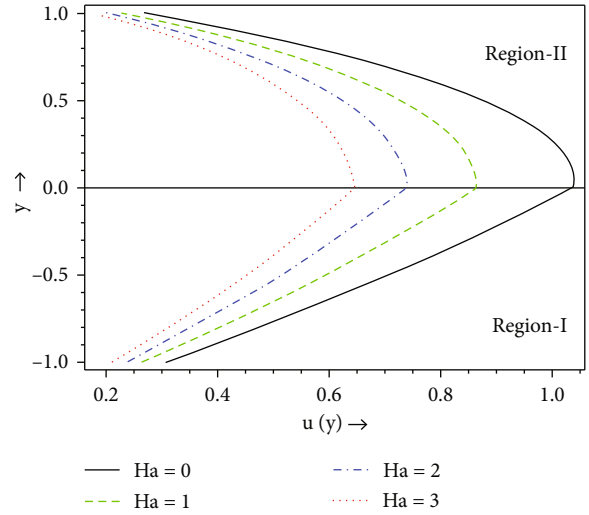

FIGURE 4: Effect of Hartmann number Ha on velocity components.

obtained in closed form. The effects of pertinent parameters on the velocity $u_1(y)$ in region I and on the velocity $u_2(y)$ in region II are studied and presented through Figures 2–12. The set of fixed values of all parameters (-
$Ha = 3$, Re = 2, P = 1.1, $n_\sigma = 1.0$, $n_\mu = 0.9$, $n_\rho = 0.9$, $a_1 = 10$, $a_2 = 10$, $\theta = \pi/4$, Da = 1, $s_1 = 2$, K = 1, and $\lambda_1 = 0.3$) is carefully chosen in accordance with previous literatures (see [30]) when a sparticular parameter is varied to see the variation. Further, if any, variation in the parameters is indicated in that particular figure.

The effect of the couple stress parameter s_1 on the velocity components is shown in Figure 2. It is seen that as $s_1 = \mu_1 h^2/\eta_1$ is increasing (i.e., as η is decreasing); the velocity components are increasing. We conclude from Figure 2 that the velocity in the case of a couple stress fluids is smaller than that in the Newtonian fluid case. Thus, the presence of couple stresses in the fluid decreases the velocity. This may be due to the fact that the couple stresses spend some energy to rotate the particles, thereby decreasing the particle velocity. We observe that the flow velocities are strongly dependent on the non-Newtonian material parameter s_1. As $s_1 \longrightarrow \infty$ ($as\, \eta \longrightarrow 0$); the velocity component $u_2(y)$ in region I corresponds to the Newtonian fluid. This particular velocity profile represents the flow of immiscible fluids (Newtonian fluid and Jeffrey fluid) in a porous medium with slip boundary conditions.

The effects of Jeffrey parameter λ_1 on the velocity profile is shown in Figure 3. It is observed that on increasing Jeffrey parameter λ_1, the velocity of the fluid in the region II increases. Further, the maximum values of fluid velocity occur at the interface for small Jeffrey parameter λ_1, and it shifts to region II for large Jeffrey parameter λ_1. This is because of the force due to shear stresses decreases when the Jeffrey parameter λ_1 increases. We observe that the fluid velocity in the region II is strongly dependent on the non-Newtonian material parameter λ_1. Further, it is seen that, as λ_1 approaches zero, the flow corresponds to that of

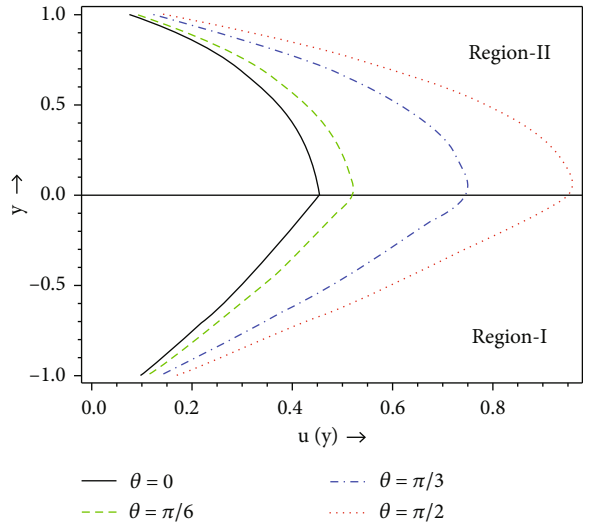

Figure 5: Variation of velocities with the angle of inclination (θ).

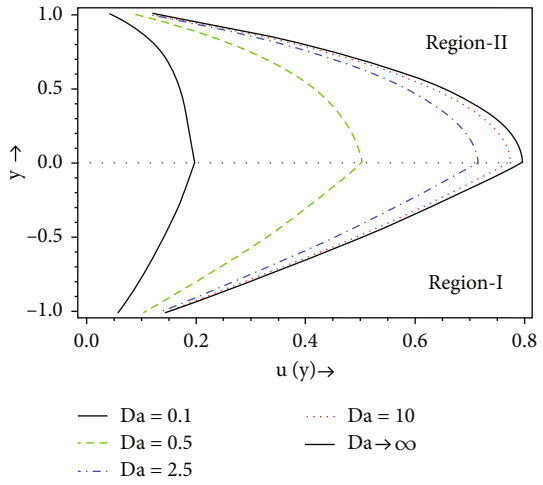

Figure 6: Effect of Darcy number $Da = k/h^2$ on velocity components.

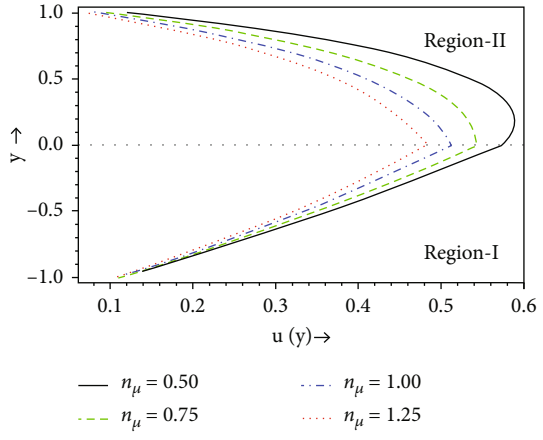

Figure 7: Effect of viscosity ratio $\eta_\mu = \mu_2/\mu_1$ on velocity components.

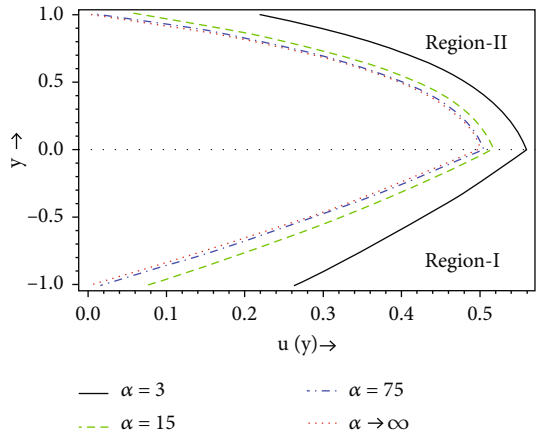

Figure 8: Effect of slip parameter $\alpha(=\alpha_1 = \alpha_2)$ on velocity components.

immiscible couple stress fluid and Newtonian fluid in a porous channel.

The effect of Hartmann number on the distribution of velocity components is as shown in Figure 4. The velocity profile attains the maximum for $Ha = 0$; this indicates the fluid flow in the absence of a magnetic field attains the maximum velocity. As Ha is increasing, it is seen that the velocity is decreasing. This shows that the imposed magnetic field has a retarding effect on the flow. Therefore, increasing the Hartmann number increases the effect of resistive force, which further decreases the flow velocity.

In Figure 5, the effect of the angle of inclination of the magnetic field on the velocity profile is shown. We observe that the velocity profile increases with the increasing of the angle inclination (θ) relative to y-axis of the applied magnetic field. This is due to the fact that the magnetic field has maximum effect in the transverse direction of the flow to retard the motion of the fluids.

From Figure 6, it is seen that as the permeability parameter $Da = k/h^2$ is increasing (i.e., as the permeability k is increasing), the velocity is increasing, and the increase of the permeability of the porous medium reduces the drag force and hence causes the flow velocity to increase. As $Da \longrightarrow \infty$, the velocity corresponds to the immiscible fluids (couple stress fluid and Jeffrey fluid) flow between two parallel plates in the absence of porous media.

The effect of the shear viscosity ratio $\eta_\mu = \mu_2/\mu_1$ is depicted in Figure 7. As η_μ is increasing, the velocity is decreasing. For $\eta_\mu < 1.00$ the velocity in region II is more than in region I. It confirms that the fluid with less viscosity has more velocity. For $\eta_\mu \geq 1.00$, the velocity components are symmetric about the interface. The maximum velocity of the fluid occurs at the interface of the regions when $\eta_\mu \geq 1.00$, while the velocity of the fluid in region II first increases and gains maximum value and then decreases toward the wall of the plate of region II.

Figure 8 shows the effect of slip parameter $\alpha = h/\beta_1 = h/\beta_2 (= \alpha_1 = \alpha_2)$ on the velocity profile. As α is increasing, the velocity is decreasing in both regions at the same rate,

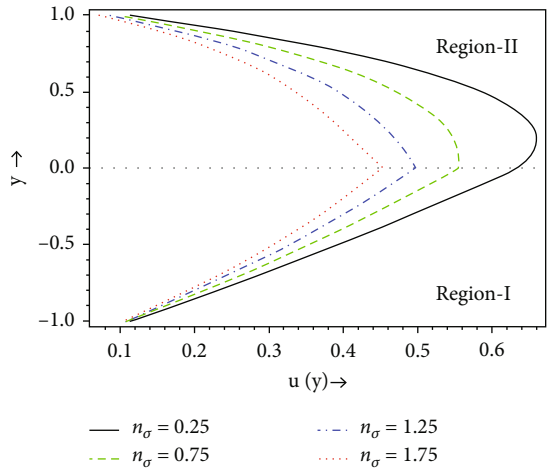

Figure 9: Variation of velocity with electrical conductivity ratio.

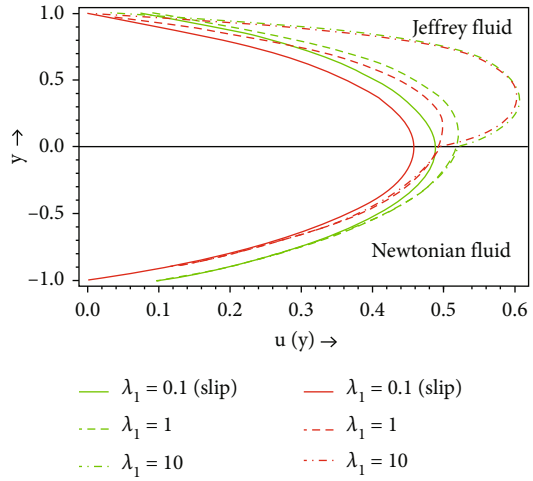

Figure 10: Variation of velocity of Newtonian and Jeffrey fluids with Jeffrey fluid parameter λ_1.

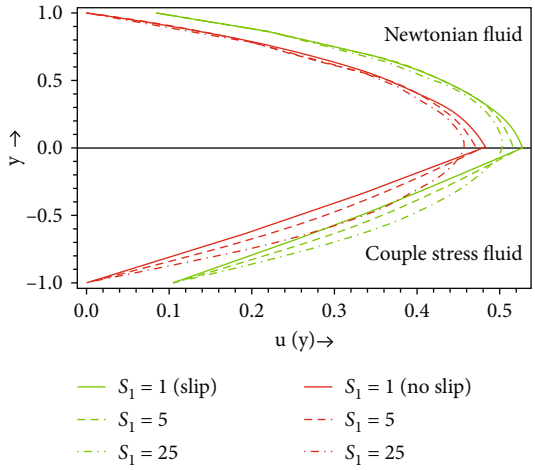

Figure 11: Velocity variation of couple stress and Newtonian fluid with couple stress fluid parameter s_1.

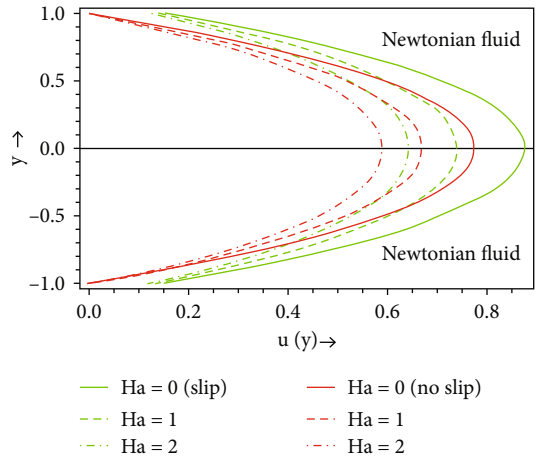

Figure 12: Velocity variation of two immiscible Newtonian fluids with Hartmann number Ha.

and hence the velocity profiles become flatten due to the decreasing shearing force from the slip boundary. Further, when $\theta = 0$ and$\alpha \longrightarrow \infty (\beta \longrightarrow 0)$ represents the flow with no-slip boundary conditions which is similar result with Devakar [5] and Pei-Ying et al. [29].

The influence of electrical conductivity ratio $n_\sigma = \sigma_2/\sigma_1$ on the velocity profile is shown in Figure 9. It is seen that the velocity of fluids in both regions decreases with the increase in the electrical conductivity ratio. The increasing in conductivity ratio means increasing the resistive force to the fluid flow. It is important to note that the velocity of the fluid in region II is greater than the velocity of the fluid in region I, and the maximum velocity occurs in region II for $n_\sigma = \sigma_2/\sigma_1 \leq 1.25$.

5.2. Limiting Cases

(i) if the couple stress parameter $s_1 \longrightarrow \infty$ or $\eta_1 = 0$, then the problem corresponds to the flow of two immiscible Newtonian fluid and Jeffrey fluid flow in the porous channel with aunifrom inclined magneticfield

(ii) if Jeffrey fluid parameter $\lambda_1 = 0$, then the problem corresponds to the flow of two immiscible couple stress and Newtonian fluids through porous channel with a unifrom inclined magnetic field

(iii) if the couple stress parameter $s_1 \longrightarrow \infty$ or $\eta_1 = 0$ and Jeffrey fluid parameter $\lambda_1 = 0$, then the problem corresponds to the flow of two immiscible Newtonian fluids flow in the porous channel with a unifrom inclined magnetic field

We present some results in the absence of couple stress and/or Jeffrey fluid parameters through Figures 10–12. In Figure 10, as the Jeffrey fluid parameter λ_1 increases, the Jeffrey fluid velocity is more than the Newtonian fluids and

Table 1: Variation of volumetric flow rate with conductivity ratio (n_σ), slip parameter (α), Hartmann number (Ha) and viscosity ratio (n_μ).

n_σ	Q	$\alpha_1 = \alpha_2 = \alpha$	Q
0.25	1.00247	5	0.8849
0.75	0.89079	10	0.84544
1.25	0.80541	15	0.82998
1.75	0.73793	25	0.8166
Ha	Q	n_μ	Q
0	1.29261	0.25	1.17604
0.5	1.18736	0.5	1.00417
1	1.09815	1	0.81588
2	0.9551	1.5	0.70028

Table 2: Variation of volumetric flow rate with Darcy number (Da), angle of inclination (θ), and Jeffery fluid parameter (λ_1).

Da	Q	θ	Q	λ_1	Q
1	0.84544	$\theta = 0$	0.63009	0	0.80975
2	0.94787	$\theta = \pi/6$	0.72176	1	0.89998
3	0.98787	$\theta = \pi/3$	1.02157	2	0.94632
4	1.00917	$\theta = \pi/2$	1.29261	3	0.97628

Table 3: Variation of shear wall stress with Hartmann number (Ha), viscosity ratio (n_μ), slip parameter (α) and conductivity ratio (n_σ) at the lower plate (τ_{xy1}) and at the upper plate (τ_{xy2}).

Ha	$\tau\ xy1$	τ_{xy2}	n_μ	$\tau_{xy}\ 1$	$\tau\ xy2$
0	1.66437	0.14376	0.25	1.27312	0.2065
0.5	1.56011	0.13341	0.5	1.25362	0.14121
1	1.47124	0.12461	0.75	1.22981	0.11125
1.5	1.39452	0.11705	1	1.20723	0.09331
α	$\tau_{xy}\ 1$	$\tau_x\ y2$	$n\ \sigma$	$\tau\ xy1$	$\tau\ xy2$
5	1.22119	-0.0722	0.25	1.2661	-0.0702
10	1.21602	-0.012	0.75	1.23056	-0.1082
15	1.21399	-0.0072	1.25	1.20312	0.00366
20	1.21291	-0.005	1.75	1.18121	0.07319

Table 4: Variation of shear stress with Jeffery fluid parameter (λ_1) and angle of inclination (θ) at the lower plate (τ_{xy1}) and at the upper plate (τ_{xy2}).

$\lambda\ 1$	$\tau\ xy1$	$\tau_{xy}\ 2$	θ	$\tau\ xy1$	$\tau\ xy2$
0	1.20383	-0.0658	0	0.99151	0.01846
1	1.23084	-0.0431	$\pi/6$	1.0882	0.01209
2	1.23899	-0.0821	$\pi/3$	1.39452	-0.0145
3	1.24184	-0.1331	$\pi/2$	1.66437	-0.0779

Table 5: Variation of shear wall stress Darcy number (Da) and density ratio ($n_{\rho)}$ at the lower plate (τ_{xy1}) and at the upper plate (τ_{xy2}).

Da	$\tau\ xy1$	τ_{xy2}	n_ρ	$\tau_{xy}\ 1$	$\tau\ xy2$
1	1.21602	-0.0323	0.5	1.15713	0.07439
2	1.32484	-0.0191	1.0	1.23074	-0.007
3	1.36709	-0.0337	1.5	1.30434	-0.1774
4	1.38956	-0.0312	2.0	1.37795	-0.3365

$\lambda_1 = 0$; the two fluids are Newtonian fluids, and hence the two velcities are symmetric with respect the fluid-fluid interface. In Figure 11 we observe the couple stress fluid velocity lesser than Newtonian fluid velocity.. The effect of Hartmann number (Ha) on the distributions of velocity profiles of the two immiscible Newtonian fluids is shown in Figure 12. As Ha increases, the velocity decreases. The velocity profiles attain maximum value for $Ha = 0$, this indicates the fluid flow in the absence of a magnetic field attains the maximum velocity. Furthermore, the profile is symmetric with respect to the fluid-fluid interface.

5.3. Flow Rate and Shear Stresses. The variations of volumetric flow rate and shear stresses on the upper and lower wall of the channel with different physical parameters are shown in Tables 1–5.

From Table 1, the volumetric flow rate in the horizontal porous channel decreases with the increase of conductivity ratio (n_σ), slip parameter (α), Hartmann number (Ha), and viscosity ratio (n_μ) in immiscible couple stress and Jeffery fluid flow. This is obvious, for example, as the magnetic parameter increases, the velocity decreases which in turn lead to the decrease in the volumetric flow rate. The effects of the other pertinent parameters on the volumetric flow rate are in tune with the velocity.

From Table 2, the volumetric flow rate in the porous channel increases with the increase of Darcy number (Da), angle of inclination (θ), and Jeffery fluid parameter (λ_1). This is obvious, for example, as Darcy number increases, the velocity increases which lead to the increase in the volumetric flow rate. The effects of the other pertinent parameters on the volumetric flow rate are in tune with the velocity.

From Table 3, the shear wall stress of immiscible couple stress and Jeffery fluid flow in the horizontal porous channel decreases with the increase magnetic field (M), viscosity ratio (n_μ), slip parameter ($\alpha = \alpha_1 = \alpha_2$), and conductivity ratio (n_σ). It is also noticed that the shear stress on the wall of the lower region is greater than the shear stress on the wall of the upper region of the horizontal porous channel.

From Table 4, with the increasing of Jeffery parameter (λ_1) and angle of inclination (θ) the shear stress is increasing at the lower wall and is decreasing at the upper wall. It is also noticed that the shear stress on the wall of the lower region is greater than the shear stress on the wall of the upper region of the horizontal porous channel.

From Table 5, the increasing of Darcy number (Da) and density ratio ($n_{\rho)}$ makes the shear stress on the wall of the

region increase and decrease in the upper region. It is also noticed that the shear stress on the wall of the lower region is greater than the shear wall stress on the wall of the upper region of the horizontal porous channel.

6. Conclusion

Effects of slip and inclined uniform magnetic field on immiscible fluids (couple stress fluid and Jeffrey fluid) flow in a porous channel are studied. We observe that, as the Hartmann number, slip parameter and viscosity ratios are increasing, the velocity components are decreasing in both regions. The velocity increases in region II as the Jeffery parameter is increasing, as the velocity in region I is constant. As the couple stress parameter is increasing, the velocity is increasing. As the Darcy number Da and the Reynolds number Re are increasing; the velocity is increasing. The shear stress on the wall of the lower region is greater than the shear stress on the wall of the upper region of the porous channel.

Appendix

A. Simplified Constants

$$C_{11} = -\frac{\left(C_{13}\lambda_{12}^2\right)}{\lambda_{11}^2},$$

$$C_{12} = -\frac{(P1 + C_{14}L_3 + C_{13}L_{15})}{L_1},$$

$$C_{13} = -\frac{H_8L_{10} - H_7L_{13}}{H_9L_{10} - L_9L_{13}L_{14}}, C_{14} = -(H_1 + C_{13}H_3)/H_2,$$

$$C_{21} = P3 + C_{13}L_{14}, C_{22} = -\frac{H_7H_9 - H_8L_9L_{14}}{H_9L_{10} - L_9L_{13}L_{14}},$$

$$P1 = \frac{\text{Re } P s_1}{m_1}, P2 = \left(\frac{n_\rho}{n_\mu m_2}\right)(1 + \lambda_1) \text{ Re } P,$$

$$P3 = P1 - P2, s$$

$$L_1 = \left(-\sinh \lambda_{11} - \frac{(\cosh \lambda_{11})\lambda_{11}}{a_1} + \frac{(\cosh \lambda_{11})\lambda_{11}^3}{a_1 s_1}\right),$$

$$L_2 = \left(\cosh \lambda_{11} + \frac{(\sinh \lambda_{11})\lambda_{11}}{a_1} - \frac{(\sinh \lambda_{11})\lambda_{11}^3}{a_1 s_1}\right),$$

$$L_3 = \left(-\sinh \lambda_{12} - \frac{(\cosh \lambda_{12})\lambda_{12}}{a_1} + \frac{(\cosh \lambda_{12})\lambda_{12}^3}{a_1 s_1}\right),$$

$$L_4 = \left(\cosh \lambda_{12} + \frac{(\sinh \lambda_{12})\lambda_{12}}{a_1} - \frac{(\sinh \lambda_{12})\lambda_{12}^3}{a_1 s_1}\right),$$

$$L_5 = (\cosh \lambda_{11})\lambda_{11}^2, L_6 = -(\sinh \lambda_{11})\lambda_{11}^2,$$

$$L_7 = (\cosh \lambda_{12})\lambda_{12}^2, L_8 = -(\sinh \lambda_{12})\lambda_{12}^2,$$

$$L_9 = \left(\cosh \lambda_{21} + \frac{(\sinh \lambda_{21})\lambda_{21}}{a_2(1 + \lambda_1)}\right),$$

$$L_{10} = \left(\sinh \lambda_{21} + \frac{(\cosh \lambda_{21})\lambda_{21}}{a_2(1 + \lambda_1)}\right), L_{11} = \left(\lambda_{11} - \frac{\lambda_{11}^3}{s_1}\right),$$

$$L_{12} = \left(\lambda_{12} - \frac{\lambda_{12}^3}{s_1}\right), L_{13} = -\frac{\eta_\eta \lambda_{22}}{1 + \lambda_1}, L_{13} = \left(1 - \frac{\lambda_{12}^2}{\lambda_{11}^2}\right),$$

$$L_{15} = \left(L_4 - \frac{L_2\lambda_{12}^2}{\lambda_{11}^2}\right), L_{16} = \left(L_7 - \frac{L_5\lambda_{12}^2}{\lambda_{11}^2}\right), H_1 = -\frac{\text{P1}L_6}{L_1},$$

$$H_2 = \left(-\frac{L_3L_6}{L_1} + L_8\right), H_3 = \left(-\frac{L_6L_{15}}{L_1} + L_{16}\right),$$

$$H_4 = -\frac{\text{P1}L_{11}}{L_1}, H_5 = \left(-\frac{L_3L_{11}}{L_1} + L_{12}\right), H_6 = -\frac{L_{11}L_{15}}{L_1},$$

$$H_7 = \text{P2} + \text{P3}L_9, H_8 = H_4 - \frac{H_1H_5}{H_2}, H_9 = \left(-\frac{H_3H_5}{H_2} + H_6\right). \tag{41}$$

Nomenclature

B_o:	Uniform magnetic field (W/m^2)
Da:	Darcy number (-)
k_i:	Permeability of porous medium (m^2)
Ha:	Hartmann number (-)
M:	Magnetic parameter (-)
n_μ:	Viscosity ratio (-)
n_σ:	Electric conductivity ratio (-)
n_ρ:	Density ratio (-)
Re:	Reynolds number (-)
s_i:	Couple stress parameters (-)
T_i:	Temperature profile (K)
u_i:	Velocity profile (m/s)
α_i:	Slip parameter (-)
μ_i:	Dynamic viscosity (kg/(m.s))
η_1:	Couple stress viscosity ((kg.m)/s)
σ_i:	Electrical conductivity (S/m)
θ:	Angle of inclination (rad)
λ_1:	Jeffrey fluids parameter (-)
β_i:	Slip coefficient (m)
ρ_i:	Density (kg/m^3)
Subscript i:	1 and 2 for region I and II.

Data Availability

No data were used to support this study.

Conflicts of Interest

The authors declare that they have no conflicts of interest.

Acknowledgments

We thank the referees for their comments which have resulted in this revised version of the paper.

References

[1] A. H. P. Skelland, *Non-Newtonian Flow and Heat Transfer*, John Wiley and Sons Inc, New York, 1966.

[2] R. P. Chhabra and J. F. Richardson, *Non-Newtonian Flow in the Process Industries; Fundamentals and Engineering Applications*, Elsevier Ltd, Butterworth Heinemann Publishers, 1999.

[3] V. Kumar Stokes, "Couple stresses in fluids," *Journal of Applied Fluid Mechanics*, vol. 9, no. 9, pp. 1709–1715, 1966.

[4] V. Kumar Stokes, *Theories of Fluids with Microstructure; an Introduction*, Springer-Verlag, Berlin, 1984.

[5] M. Devakar, D. Sreenivasu, and B. Shankar, "Analytical solutions of couple stress fluid flows with slip boundary conditions," *Alexandria Engineering Journal*, vol. 53, no. 3, pp. 723–730, 2014.

[6] F. Ahmad, M. Nazeer, W. Ali et al., "Analytical study on couple stress fluid in an inclined channel," *Scientia Iranica B*, vol. 28, no. 4, pp. 2164–2175, 2021.

[7] S. Jangili, S. Olumide Adesanya, H. Abiodun Ogunseye, and R. Lebelo, "Couple stress fluid flow with variable properties: a second law analysis," *Mathematical Methods in the Applied Sciences*, vol. 42, no. 1, pp. 85–98, 2019.

[8] B. Reddappa, S. Sreenadh, K. Kumarasway Naidu, and A. Parandhama, "Poiseuille flow of conducting jeffrey fluid between parallel plates when one of the walls is provided with porous lining," *Journal of Ultra Scientist of Physical Sciences*, vol. 28, no. 1, 2016.

[9] N. Akbar, Z. Hayat Khan, and S. Nadeem, "Influence of magnetic field and slip on jeffrey fluid in a ciliated symmetric channel with metachronal wave pattern," *Journal of Applied Fluid Mechanics*, vol. 9, no. 2, pp. 565–572, 2016.

[10] S. Akram and S. Nadeem, "Influence of induced magnetic field and heat transfer on the peristaltic motion of a Jeffrey fluid in an asymmetric channel: closed form solutions," *Journal of Magnetism and Magnetic Materials*, vol. 328, pp. 11–20, 2013.

[11] R. Shail, "On laminar two-phase flows in magnetohydrodynamics," *International Journal of Engineering Science*, vol. 11, no. 10, pp. 1103–1108, 1973.

[12] H. I. Meyer and A. O. Garder, "Mechanics of two immiscible fluids in porous media," *Journal of Applied Physics*, vol. 25, no. 11, pp. 1400–1406, 1954.

[13] R. N. Bhattacharya, "The flow of immiscible fluids between rigid plates with a time dependent pressure gradient," *Bulletin of the Calcutta Mathematical Society*, vol. 1, pp. 129–137, 1968.

[14] S. Berg, A. W. Cense, J. P. Hofman, and R. M. M. Smits, "Two-phase flow in porous media with slip boundary condition," *Transport in Porous Media*, vol. 74, no. 3, pp. 275–292, 2008.

[15] M. P. Devi and S. Srinivas, "Thermal characteristics on two immiscible fluid flows in a porous space with time dependent pressure gradient," *Proceedings of the Institution of Mechanical Engineers, Part E: Journal of Process Mechanical Engineering*, 2022.

[16] Y. Kumar Yadav and J. Sneha, "Influence of an inclined magnetic field on the poiseuille flow of immiscible micropolar-newtonian fluids in a porous medium," *Canadian Journal of Physics*, vol. 96, no. 9, pp. 1016–1028, 2018.

[17] Y. K. Yadav and J. Sneha, "Influence of magnetic field on the Poiseuille flow of immiscible Newtonian fluids through highly porous medium," *Journal of the Brazilian Society of Mechanical Science and Engineering*, vol. 42, no. 4, 2020.

[18] I. A. Ansari and S. Deo, "Effect of magnetic field on the two immiscible viscous fluids flow in a channel filled with porous medium," *National Academy Science Letters*, vol. 40, no. 3, pp. 211–214, 2017.

[19] A. Matias, O. Bautista, F. Méndez, and P. Escandón, "Electro-osmotic pumping between two immiscible electrical conducting fluids controlled by interfacial phenomena," *Journal of Applied Fluid Mechanics*, vol. 11, no. 3, pp. 667–678, 2018.

[20] M. S. Malashetty and J. C. Umavathi, "Two-phase magnetohydrodynamic flow and heat transfer in an inclined channel," *International Journal of Multiphase Flow*, vol. 23, no. 3, pp. 545–560, 1997.

[21] J. V. Ramana Murthy and J. Srinivas, "Thermal analysis of a flow of immiscible couple stress fluids in a channel," *Journal of Applied Mechanics and Technical Physics*, vol. 57, no. 6, pp. 997–1005, 2016.

[22] B. Punnamchandar and Y. S. Fekadu, "Effects of slip and uniform magnetic field on flow of immiscible couple stress fluids in a porous medium channel," *The International Journal of Engineering and Science*, vol. 1, pp. 1–8, 2020.

[23] P. A. Thompson and S. M. Troian, "A general boundary condition for liquid flow at solid surfaces," *Nature*, vol. 389, no. 6649, pp. 360–362, 1997.

[24] S. Akram, M. Athar, K. Saeed, and A. Razia, "Impact of slip on nanomaterial peristaltic pumping of magneto-Williamson nanofluid in an asymmetric channel under double-diffusivity convection," *Pramana*, vol. 96, no. 1, pp. 1–13, 2022.

[25] P. Bitla and T. K. V. Iyengar, "Effects of slip on pulsating flow of an incompressible micropolar fluid through a porous medium between two parallel plates," *Journal of Porous Media*, vol. 16, no. 8, pp. 769–775, 2013.

[26] E. A. Ashmawy, "Unsteady stokes flow of a couple stress fluid around a rotating sphere with slip," *The European Physical Journal Plus*, vol. 131, no. 5, pp. 1–8, 2016.

[27] D. Srinivasacharya and K. H. Bindu, "Entropy generation due to micropolar fluid flow between concentric cylinders with slip and convective boundary conditions," *Ain Shams Engineering Journal*, vol. 9, no. 2, pp. 245–255, 2018.

[28] L. L. Ferrás, J. M. Nóbrega, and F. T. Pinho, "Analytical solutions for Newtonian and inelastic non-Newtonian flows with wall slip," *Journal of Non-Newtonian Fluid Mechanics*, vol. 175-176, pp. 76–88, 2012.

[29] P. Y. Xiong, M. Nazeer, F. Hussain et al., "Two-phase flow of couple stress fluid thermally effected slip boundary conditions: numerical analysis with variable liquids properties," *Alexandria Engineering Journal*, vol. 61, no. 5, pp. 3821–3830, 2022.

[30] K. Ramesh, "Influence of heat transfer on Poiseuille flow of MHD Jeffrey fluid through porous medium with slip boundary conditions," in *AIP conference proceedings*, vol. 1860, 2017no. 1.

[31] P. D. Selvi, S. Sreenadh, E. Kesava Reddy, and G. Gopi Krishna, "Viscous flow of Jeffrey fluid in an inclined channel through deformable porous media," *World Applied Sciences Journal*, vol. 35, no. 5, pp. 669–677, 2017.

[32] D. Kumar and M. Agarwal, "Flow of two immiscible viscous fluids in porous medium between two parallel plates," *Ganita*, vol. 67, no. 1, pp. 61–71, 2017.